Analyst

TUTORIAL REVIEW

View Article Online
View Journal | View Issue

CrossMark click for updates

Cite this: *Analyst*, 2016, **141**, 1611

Gold nanoparticles as sensitive optical probes

Zhiqin Yuan,*[a] Cho-Chun Hu,[b] Huan-Tsung Chang*[c] and Chao Lu[a]

Received 28th December 2015,
Accepted 26th January 2016

DOI: 10.1039/c5an02651b

www.rsc.org/analyst

Gold nanoparticles (Au NPs) have become one of the most popular materials for sensing of analytes of interest in the last decade, mainly because of their ease in preparation and conjugation, stability, biocompatibility, and size-dependent optical properties. We have witnessed many sensitive and selective Au NP based optical systems for the quantitation of metal ions, anions, proteins, and DNA, based on analyte induced changes in their absorption, fluorescence, and scattering. In this tutorial review, we briefly discuss wet chemical approaches for the preparation of Au NPs. Sensing mechanisms and strategies of Au NP based optical systems are provided to show basic concepts in designing sensitive and selective sensing systems. Strategies for signal amplification applied in Au NP based systems are emphasized for the analysis of trace amounts of analytes in real samples. Many excellent Au NP based optical sensing systems are discussed to highlight their practicality for the analysis of complicated biological and environmental samples. The tutorial review ends with the discussion of the challenges and future trends of Au NP based optical sensing systems.

Introduction

Quantitation of analytes of interest from real samples is important in many fields such as medical, environmental, material, pharmaceutical and food sciences.[1,2] To develop highly sensitive and selective sensing systems, probes having high affinity toward analytes of interest and large signal changes induced by the analytes are required. Although a number of organic and biochemical probes have been applied successfully to quantitation of various analytes, they are sometimes limited by complicated preparation/fabrication processes of the probes, sophisticated and costly detection systems and/or the requirement of highly costly reagents. Therefore, simple, cost-effective, sensitive and selective probes for the quantitation of chemical and/or biological analytes from complicated samples are in demand.

Nanomaterials have special physicochemical properties that offer a suitable platform for the design of sensitive and selective sensing systems for various analytes through integrating nanotechnology and biotechnology.[3,4] Gold nanoparticles

[a]*State Key Laboratory of Chemical Resource Engineering, Beijing University of Chemical Technology, Beijing 100029, China. E-mail: yuanzq@mail.buct.edu.cn; Tel: +86-10-64411957*
[b]*Department of Applied Science, National Taitung University, Taitung 95002, Taiwan*
[c]*Department of Chemistry, National Taiwan University, 1, Section 4, Roosevelt Road, Taipei 106, Taiwan. E-mail: changht@ntu.edu.tw; Fax: +1-886-2-33661171; Tel: +1-886-2-33661171*

Zhiqin Yuan

Zhiqin Yuan is currently a school specially appointed Associate Professor of State Key Laboratory of Chemical Resource Engineering, Beijing University of Chemical Technology. He obtained his PhD from College of Chemistry and Chemical Engineering, Hunan University, in 2013 with Dr Yan He and Dr Edward S. Yeung. His research interests are focused on the synthesis and analytical applications of metal nanoparticles and nanoclusters.

Cho-Chun Hu

Cho-Chun Hu is currently an Associate Professor of the Department of Applied Science, National Taitung University. He received his PhD from the Department of Chemistry, National Taiwan University, in 1995 with Dr Chuen-Ying Liu. His major interest is to understand important chemical processes in analytical chemistry, synthesis of nanomaterials and polymer chemistry.

(Au NPs) have been extensively studied in many fields like analytical chemistry because of their unique optical, electrical and catalytic properties, which can be readily controlled by varying their size, shape, composition and surrounding environment.[5] The simple preparation, excellent biocompatibility, wide surface conjugation chemistry, as well as the attractive plasmonic coupling of Au NPs make them excellent candidates for the development of probes for numerous analytes with desired properties.[6–8] The high surface-to-volume ratio of Au NPs allows their multifunctionalization *via* assembling multiple organic or biological ligands onto their surfaces, which strengthens their interactions with target analytes and enhances their capability for real-time multiplex analysis of multiple targets.[9,10] Various detection modes such as absorption, fluorescence, and surface enhanced Raman scattering (SERS) are commonly used in developing Au NP based sensing systems.[11–13] These systems have shown that Au NPs are ideal for developing simple, sensitive, selective and cost-effective sensing systems for the quantitation of various target analytes in environmental and biological samples.[12]

Although many excellent review articles on Au NP based sensing systems have been published in the past decade,[7–15] a tutorial review will facilitate junior researchers (potential users) to understand the fundamental principles and to select a proper system for the analysis of samples of interest. In this tutorial review, the syntheses and properties of Au NPs are discussed briefly. Optical sensing systems using Au NPs, including absorption, fluorescence and SERS, are provided, emphasizing their sensing strategies/mechanisms. Recent advances in Au NP based optical sensing systems for various analytes, including ions, small molecules and biopolymers, are provided to show their practicality in the analysis of biological and environmental samples. Owing to a space limit in this review article, only a few examples are selected to highlight the potential use of Au NPs in sensing and cell imaging. Current challenges and future outlooks of Au NP based sensors for real-time and high-throughput analysis of complex biological and environmental samples are discussed based on our experience in developing Au NP based optical systems.

Brief overview of Au NPs

Syntheses of Au NPs

Numerous physical and chemical methods for the synthesis of Au NPs have been reported, and much effort has been dedicated to the synthesis of Au NPs with controllable size, stability and functionality during the last two decades.[5,16] Nevertheless, the wet chemical approach has overwhelmingly attracted growing attention because of their advantages over physical methods with respect to scalability, reproducibility, and versatility.[17] The synthesis of Au NPs with different sizes and functionality is well established through wet-chemistry in both aqueous and organic solutions.

Citrate reduction. In a typical synthesis proposed by Turkevich in 1951, Au salts are reduced by adding citrate as a reducing agent, leading to the nucleation to form seeds and then growth of the seeds to form NPs.[18] To reduce local concentration of gold ions (Au^{3+}) and to accelerate the reaction speed, the reaction is often conducted under high-speed stirring at 100 °C. The as-formed Au NPs are stabilized by charged citrate ions as a stabilizing agent. By controlling the molar ratio of sodium citrate to Au^{3+}, Au NPs with controllable sizes can be prepared; for example, Au NPs with a size of 13 nm can be prepared at the citrate/Au^{3+} molar ratio of 3.88.[19] At a high citrate/Au^{3+} molar ratio, nucleation is dominant, leading to the formation of small size Au NPs. On the other hand, large size Au NPs are formed at a low citrate/Au^{3+}, mainly because the growth of Au seeds becomes dominant. Having advantages of simplicity and reproducibility, this method is most commonly applied to the preparation of Au NPs with sizes ranging from 5 to 100 nm.

Brust–Schiffrin method. To obtain small Au NPs (<5 nm), a strong reducing agent such as sodium borohydride is usually

Huan-Tsung Chang

Huan-Tsung Chang is currently a Professor of the Department of Chemistry, National Taiwan University. He is a fellow of the Royal Society of Chemistry. He obtained his PhD from the Department of Chemistry, Iowa State University, in 1994 with Dr Edward S. Yeung. His current research interests include nanotechnology, green chemistry, biosensors, and mass spectrometry.

Chao Lua

Chao Lu received his PhD degree in Materials Science from Chinese Academy of Sciences with Dr Jin-Ming Lin in 2004. He is currently a full professor of State Key Laboratory of Chemical Resource Engineering, Beijing University of Chemical Technology. In 2011, he was selected to participate in the 'New Century Outstanding Talent' scheme of the Ministry of Education. His research is focused on the synthesis and characterization of nanostructured materials, the fabrication of luminescent films and nanosensors, and chemiluminescence.

needed. Although small Au NPs (3.5 nm) can be produced by using sodium borohydride, the trend of aggregation of the as-prepared Au NPs limits their storage and further application. By taking advantage of the strong thiol–gold bonding, Brust and Schiffrin developed a two-phase synthetic strategy to synthesize small and stable Au NPs.[20] Using a surfactant such as tetraoctylammonium bromide, Au salt is firstly transferred from the aqueous phase to toluene, in which they are reduced by sodium borohydride in the presence of a thiolate compound such as dodecanethiol. Unlike in a citrate mediated reduction, a quick solution color change from yellow/orange to brown appears within one minute after the addition of sodium borohydride. The size of as-formed Au NPs is usually in the range of 1.5–5 nm. Because of the thiolate ligand shell formed through strong thiol–gold interactions on the surface of each Au core, these Au NPs show superior stability.

Fluorescent Au NPs. Various types of fluorescent Au NPs have been synthesized in the presence of thiolates, polymers and biomacromolecules (*e.g.*, amino acids, peptides, proteins and DNAs).[21,22] Generally, the synthetic routes can be classified into two categories: bottom-up and top-down methods.[23] In the bottom-up method, fluorescent Au NPs are formed through chemical reduction or photoreduction of Au^{3+} in the presence of ligands/scaffolds that have strong interaction with Au atoms/ions and thus can stabilize as-formed Au NPs. For example, glutathione is used as a ligand to prepare fluorescent Au NPs in the absence or presence of another reducing agent (*e.g.*, carbon monoxide).[24,25] In the top-down approach, non-fluorescent Au NPs are prepared first. Etching ligands such as thiolates, polymers and DNAs are then added to etch the non-fluorescent Au NPs to form fluorescent Au NPs. For instance, 11-mercaptoundecanoic acid has been used to etch tetrakis-(hydroxymethyl)phosphonium chloride protected Au NPs to form green-emissive fluorescent Au NPs.[26,27]

Localized surface plasmon resonance of Au NPs

One of the most interesting optical properties of Au NPs is their localized surface plasmon resonance (LSPR), which results from the resonant oscillation of conduction electrons at the Au NP surface with the incident electromagnetic field.[28] The LSPR contains absorption and scattering, and thus extinction instead of absorbance is used in most studies. The electromagnetic field at the Au NP surface allows enhanced optical properties, leading to an extremely high extinction coefficient of the LSPR band that is generally several orders of magnitude larger than that of traditional organic dyes.[29] The LSPR resonance of Au NPs is located in the visible range, leading to their bright colors. The high extinction coefficient and the bright color lead to development of versatile Au NP based optical sensing systems.[13]

The LSPR of Au NPs is largely affected by the particle size, interparticle distance and local environment.[14] For instance, the maximum LSPR absorption wavelength is related to the diameter of Au NPs, mainly because increased Au NP size causes the decrease of discrete energy gaps.[30] In addition, the number of conduction electrons increases with increasing particle size, leading to higher extinction coefficient and stronger scattering intensity of larger Au NPs. The interparticle distance dependence of LSPR is through the interparticle plasmon coupling effect. Therefore, aggregation of Au NPs results in dramatic red-shifts in their absorption spectra and thus changes in the solution color from red to blue. Mie *et al.* elucidated the origin of LSPR by solving Maxwell's electromagnetic equation based on a spherical particle model in a magnetic field.[31] According to the equation, the refractive index can also affect the electromagnetic field appearing on the Au NP surface, resulting in changes in the LSRP properties of Au NPs. Thus, LSPR properties of Au NPs depend on the solution composition and ionic strength, as well as surface ligands. Consequently, Au NP based sensing systems are commonly developed through analyte induced changes in their particle size, interparticle distance and/or local environment.

Colorimetric assays

The aggregation of Au NPs results in color changes of the colloid solution from red to blue, while redispersion of the aggregated Au NPs leads to a color recovery from blue to red. The color change during Au NP aggregation or redispersion provides a general platform for absorption-based colorimetric detection of analytes that can induce the Au NP aggregation or redispersion directly or indirectly. Having an extremely high extinction coefficient and a strong interparticle distance-dependent LSPR absorption property, Au NPs are ideal for colorimetric assays. Moreover, the readout of Au NP based assays can be recorded with a UV-vis spectrophotometer or even observed by the naked eye. Accordingly, a lot of Au NP based colorimetric chemo/biosensors for the detection of inorganic ions, small molecules, oligonucleotides and proteins have been successfully fabricated based on three categories: aggregation induced colorimetric detection, disassembly mediated colorimetric sensing and colorimetric assays on single Au NPs.[7,12,14]

Aggregation induced colorimetric detection

DNA. Targets can trigger the aggregation of Au NPs directly or indirectly, resulting in a red shift of the absorption wavelength in the visible region and thus a colloid solution color change from red to blue. DNA mediated Au NP assembly was demonstrated by Mirkin *et al.*, and this character was applied to colorimetric DNA detection later with a classical sandwich design.[32] Using this strategy, two thiolated single-stranded DNA (ssDNA) were conjugated onto the surface of Au NPs through strong Au–S interactions. Target DNA induces the formation of double stranded DNA (dsDNA) through its hybridization with the two ssDNA on the surfaces of Au NPs, resulting in the generation of large Au NP aggregates and dramatic color changes (Fig. 1a).[33] Based on this sensing mechanism, many sensitive and selective assays for the quantitation of DNA have been demonstrated in the last three years.[34,35] For example, Kaposi's sarcoma and Bartonella DNA could be detected using thiolated DNA functionalized Au NPs with LODs of 2 and 1 nM, respectively.[36,37] Recent studies show the existence of

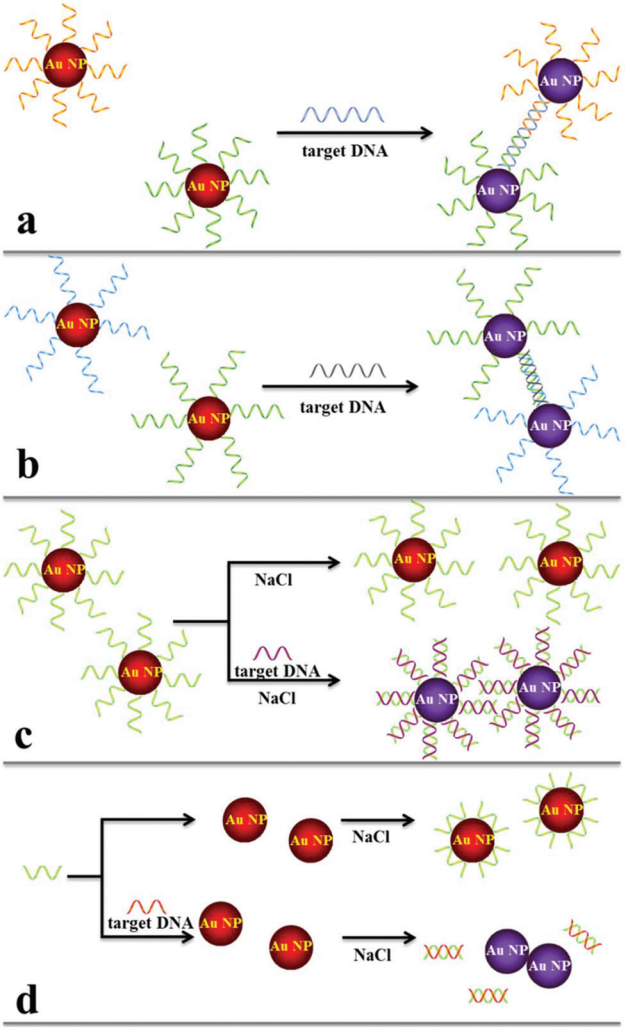

Fig. 1 Schematics of colorimetric DNA hybridization detection systems. Duplex (a) and triplex (b) DNA crosslinking and non-crosslinking of (c) thiolated DNA–Au NPs and (d) non-thiolated DNA and Au NP.

triplex DNA beyond dsDNA and ssDNA.[38] This specific DNA conformation has been used for developing Au NP based sensing systems for DNA detection.[39,40] Target DNA hybridizes with two ssDNA probes to form a triplex DNA structure, causing the Au NP aggregation and the corresponding solution color change (Fig. 1b).[41] By taking advantage of the fact that dsDNA over ssDNA exhibits a stronger salting-out effect, sensitive colorimetric DNA sensing systems have been developed based on non-crosslinking DNA hybridization (Fig. 1c).[42] However, the opposite behavior was observed with decreased density of surface ssDNA. That is, the stability of functionalized Au NPs with low ssDNA density in high ionic strength solution becomes better after hybridization.[43] Since non-thiolated ssDNA shows high affinity for citrate protected Au NP due to base-gold affinity and electrostatic forces,[44,45] non-thiolated ssDNA functionalized Au NPs exhibit high stability in high-ionic-strength solution (*e.g.*, 120 mM NaCl). Interestingly, Rothberg *et al.* found that adding complementary DNA results in the formation of dsDNA that has negligible affinity toward Au NPs, leading to the aggregation of Au NPs (Fig. 1d). On the basis of this finding, they developed a label free colorimetric DNA detection method using bare Au NPs and ssDNA.[46] This strategy does not require the attachment of ssDNA onto the surface of Au NP, and the change of the solution color takes place in less than 1 min because of the ultrafast binding of ssDNA and Au NP. Liu *et al.* demonstrated that a reduction of pH can reduce the charge repulsion between ssDNA and Au NPs and accelerates the adsorption kinetics of ssDNA.[47] On the basis of this phenomenon, they reported a facile method for instantaneous attachment of thiolated DNA to Au NPs using a low pH buffer (Fig. 2).[48,49] The whole process takes just a few minutes, and the DNA adsorption can be quantitated. Addition of target DNA leads to the formation of dsDNA and the occurrence of Au NP aggregation.[50,51] The simple sensing mechanism has been applied for the detection of dengue gene and viral RNA, with high sensitivity (down to 120 nM and 2 ng mL^{-1}) and selectivity.[52,53]

Having high specificity of base-pair hybridization and high extinction coefficient of Au NPs, DNA–Au NP based sensing systems provide selective DNA detection with LODs at the nanomolar and even subnanomolar levels. However, these assays are not sensitive enough for the analysis of disease related genes with concentrations usually ranging from attomolar to picomolar. To further improve the detection sensitivity, polymerase chain reaction (PCR) amplification is generally applied to amplify the concentration of the target gene.[4] Typically, the target DNA serves as primers/templates for DNA replication in the presence of DNA polymerase. The resulting DNA number increases in an exponential manner with the amplification cycle, allowing highly sensitive DNA detection in femtomolar and even attomolar levels. In combination with PCR and Au NPs, many sensing systems have been developed for the quantitation of disease related genes, *i.e.*, anthrax.[54] A colorimetric assay in conjunction with a resonance light scattering technique provides a LOD of 10 pM for DNA, showing a potential for the analysis of single nucleotide polymorphisms in breast cancer.[55]

Another way to improve DNA detection sensitivity is through the control of the size of Au NP aggregates. Huge aggregates lead to precipitation of Au NPs and a decrease of absorbance, diminishing the sensitivity. To overcome this

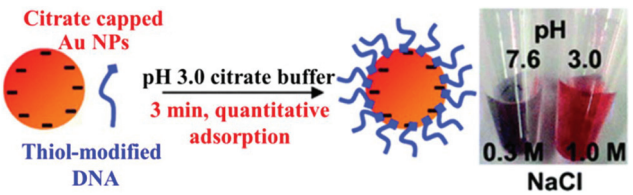

Fig. 2 Schematic illustration of attaching negatively charged thiolated DNA to negatively charged Au NPs using the low pH assisted method. Reprinted with permission from ref. 48. Copyright 2012, American Chemical Society.

problem, Chen *et al.* designed a Janus Au NP based colorimetric system with high sensitivity and a wide dynamic range.[56] The Janus Au NP possesses an asymmetrical surface that allows the formation of dimers rather than large aggregates and a reduction of the interparticle distance, providing picomolar sensitivity.

Proteins. The presence of irregular protein concentrations or protein alternation may be associated with diseases such as atherothrombosis and Alzheimer's disease, thereby precise and rapid protein detection is of great importance in proteomics and diagnostics.[57,58] A diverse range of ligand functionalized Au NPs have been reported for the detection of proteins based on protein–ligand binding-induced Au NP aggregation, protein-catalyzed ligand cleavage/polymerization-induced Au NP aggregation or protein-promoted generation of product-induced Au NP aggregation/growth.[7,14,59–61] For example, a series of carbohydrate functionalized Au NPs have been prepared for detecting carbohydrate binding proteins such as communis agglutinin 120 and lectins.[62,63] Through the specific interaction of biotin with streptavidin, biotin modified Au NPs were used for the detection of streptavidin with a LOD of 24 nM.[64] Protein functionalized Au NPs have been exploited for the detection of various proteins through the specific protein–protein interaction (*i.e.*, antigen–antibody reaction).[65,66] For example, troponin I antigen, anti-*Listeria monocytogenes* monoclonal antibodies and anti-HIV-1 p24 monoclonal antibody functionalized Au NPs were used for the detection of cardiac troponin I, *Listeria monocytogenes*, HIV-1 p24 antigen, with LODs of 15 pg mL^{-1}, 3.5 CFU mL^{-1} and 1.49 pg mL^{-1}, respectively.[67–69] On the basis of aptamer–protein interactions, Chang *et al.* achieved a sensitive detection of platelet derived growth factors (PDGFs) using aptamer–Au NP probes.[70] Combining aptamer modified Au NPs (13 nm) and fibrinogen adsorbed Au NPs (56 nm), they realized PDGF detection with improved sensitivity at the picomolar level.[71] Such an aptamer-mediated recognition strategy has also been used for sensing other proteins like thrombin.[72]

Proteases are special proteins that can selectively catalyze the hydrolysis or polymerization of their substrates, including peptides, proteins and DNA. Therefore, substrate stabilized Au NPs can act as reporters for the analysis of proteases such as phosphatase, thrombin and trypsin.[73–75] Proteases catalyze the hydrolysis or polymerization of surface substrates and diminish the stability of Au NPs, thereby inducing aggregation of Au NPs and changes in the color of the solution from red to blue. For instance, Chang *et al.* disclosed a novel and label-free colorimetric assay for selective and sensitive detection of thrombin using fibrinogen modified Au NPs.[72] Fibrinogen conjugates and stabilizes Au NPs through electrostatic and hydrophobic interactions, but adding thrombin in the presence of excess fibrinogen induced the formation of insoluble fibrillar fibrin–Au NP aggregates through the polymerization of the unconjugated and conjugated fibrinogen. The high catalytic performance allowed highly sensitive thrombin detection with a LOD of 0.04 pM. They also applied this system to plasmin detection based on plasmin mediated cleavage of fibrin structures, with a LOD of 0.4 nM in serum. The idea has been applied to the detection of other proteins, including adenosine deaminase, methyltransferase and acetyltransferase.[76–78]

Some of hydrolysis products can cause aggregation of citrate stabilized Au NPs directly, which can be transformed into a color change of Au NPs solution. In the light of this principle, acetylcholinesterase was easily detected using Au NPs.[79] Acetylcholinesterase catalyzes acetylthiocholine to produce thiocholine, which binds to the citrate Au NP surface *via* Au–S interactions and induces Au NP aggregation through electrostatic attraction. Similarly, *S*-adenosylhomocysteine hydrolase was detected using fluorosurfactant-capped Au NPs and *S*-adenosylhomocysteine, with a LOD of 6 nM.[80] Hydrolysis of *S*-adenosylhomocysteine in the presence of *S*-adenosylhomocysteine hydrolase yields homocysteine and subsequently causes the aggregation of the functional Au NPs.

To improve the sensitivity for the detection of proteins (enzymes), exonuclease-assisted cascaded recycling amplification has been applied for developing Au NP based sensing systems.[81,82] Without the addition of exonuclease, two ssDNA probes hybridize and form dsDNA, resulting in the aggregation of Au NPs. Adding exonuclease digests the formed dsDNA and releases the individual Au NPs into solution. As a consequence, the solution color turns from blue to red. TATA binding protein can form a complex with dsDNA and inhibit its digestion. This colorimetric assay provides a LOD of 10 nM for TATA binding protein.[81] With the assistance of magnetic nanoparticles, highly sensitive (LOD, 5.6 pM) thrombin detection was achieved by applying a similar strategy.[82]

Small analytes. Functional Au NPs have been used for the quantitation of various small analytes, including organic molecules, anions and cations.[83–85] Cysteamine functionalized Au NPs were used for the visualization of trinitrotoluene at the picomolar level through the donor–acceptor interaction between cysteamine and trinitrotoluene.[86] The analyte induced the aggregation of cysteamine functionalized Au NPs, resulting in a significant solution color change from red to purple. Based on a similar sensing mechanism, the positively charged Au NPs were also applied to colorimetric detection of melamine in milk products, eggs and feeds.[87] By reducing cysteine stimulated Au NP aggregation in 4-(2-hydroxyethyl) piperazine-1-ethanesulfonic acid buffer solution at pH 7.0, a sensitive colorimetric method was developed for the detection of hydrogen peroxide.[88] Polyethyleneimine modified Au NPs containing copper ions and hemin on their surfaces were used for colorimetric monitoring of β-amyloid peptides *via* the formation of a copper-β-amyloid peptides–hemin complex.[89] Using antigen functionalized Au NP probes, an immunochromatographic assay was developed for the simultaneous screening of five antibiotics in milk, including lincomycin, gentamicin, kanamycin, streptomycin and neomycin, with cutoff values for the strip test of 25, 25, 50, 50 and 100 ng mL^{-1}, respectively.[90] Aptamers functionalized Au NPs are sensitive and selective for the detection of small analytes based on the specific interaction of the aptamer with its corres-

ponding analyte.[91] Aptamer functionalized Au NPs were used for the detection of adenosine through the formation of an intact aptamer tertiary structure and thus aggregation of Au NPs.[92] By taking different stabilities of aptamer functionalized Au NPs in various solutions, sensitive (LOD, 10 nM) and selective detection of adenosine triphosphate (ATP) was demonstrated.[93] Although aptamer functionalized Au NPs are more stable than citrate stabilized Au NPs, they are unstable in solution containing 300 mM NaCl. Once ATP interacts with the aptamer, the surface negative charged density increases, leading to greater repulsion among the functional Au NPs. As a result, the functional Au NPs become more stable in the presence of ATP. More recently, other aptamer functionalized Au NPs have been demonstrated for the detection of various analytes, including abrin, 17β-estradiol and bisphenol A.[94–96] During the target recognition process, aptamers usually undergo a conformation change, which alters the binding affinity between DNA and Au NPs. Liu *et al.* developed a non-DNA attached approach for colorimetric thallium ion (Ti^{+}) sensing with a LOD of 59 μM using Ti^{+}-selective aptamers and Au NPs.[97] Aptamer molecules adsorb onto the surface of Au NPs and stabilize them in salt solution. However, the addition of Ti^{+} changes the conformation of Ti^{+}-selective aptamers from a coiled form to a quadruplex structure that has negligible affinity for Au NPs, leading to aggregation of Au NPs in salt solution.

Chemical reaction mediated Au NP assembly has been applied in sensing of small molecules, with advantages of sensitivity, selectivity and rapidity.[98,99] Thiolated active ester and phenylboronic acid functionalized Au NPs were used for colorimetric detection of dopamine through analyte induced aggregation of Au NPs.[100] More recently, thiolated azido derivatives and active ester cofunctionalized Au NPs (AE-Au NPs) were prepared for colorimetric detection of hydrogen sulfide (H_2S), with a LOD of 0.2 μM.[101] The azide groups on the surface of each AE-Au NP were reduced to form primary amines by H_2S. The as-formed amines then interacted with the active esters through a crosslinking reaction, inducing the aggregation of Au NPs (Fig. 3). The AE-Au NP based nanosensors possess high selectivity towards H_2S over other anions and thiols due to the specific azide–H_2S chemistry.

Heavy metal ions such as mercury (Hg^{2+}), lead (Pb^{2+}) and copper (Cu^{2+}) can cause damage to organisms and even nervous systems, and thus sensitive and selective approaches for their detection are of great importance. A large number of Au NP-based colorimetric systems have been developed for sensing of heavy metal ions based on coordination chemistry, aurophilic interactions and specific chemical reactions.[6,102] For example, thiolated ligand or DNA modified Au NPs have been utilized for the colorimetric Hg^{2+}, Pb^{2+} and Cu^{2+} detection through ligand–metal coordination.[6] In particular, colorimetric detection of Hg^{2+} using DNA functionalized Au NPs based on thymine–Hg^{2+}–thymine coordination chemistry has been widely studied.[103] Without the addition of Hg^{2+}, thymine rich ssDNA adsorbs onto the surfaces of Au NPs and stabilizes them in saline solution through electrostatic repulsions. However, introduction of Hg^{2+}

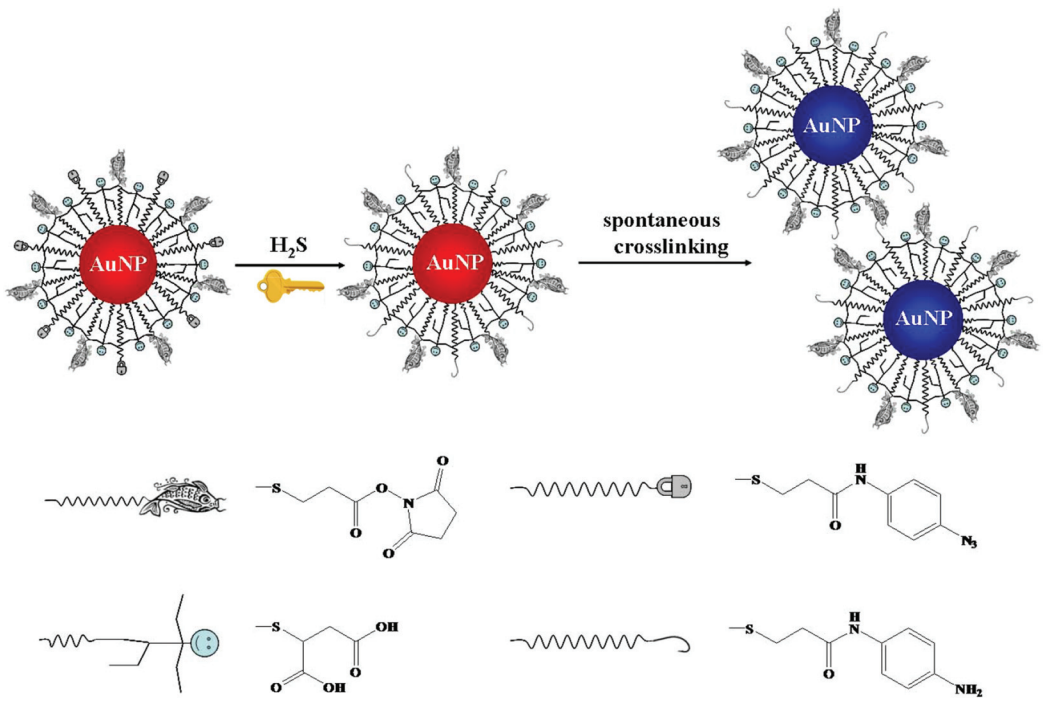

Fig. 3 Schematic representation of the sensing principle of AE-Au NP probes for the detection of H_2S. Reprinted with permission from ref. 101. Copyright 2015, American Chemical Society.

induces the conformation change of thymine rich ssDNA and reduces the surface negative charged density, resulting in aggregation of the functional Au NPs. Combining this system with a paper device, an on-field colorimetric Hg^{2+} sensing platform was developed, with a LOD of 50 nM, which is ~5 times lower than that obtained by using a conventional DNA–Au NP strategy.[104] Ligands containing amino or carboxy groups have been used to functionalize Au NPs, which have been shown to be sensitive and selective for sensing of Hg^{2+} *via* ligand–Hg^{2+} coordination.[102,105,106] Similar sensing mechanisms have been applied to the detection of Pb^{2+} and Cu^{2+} using ligands such as glutathione and cysteamine that recognize the analytes to functionalize Au NPs, with LODs of 0.1 and 0.4 μM, respectively.[107,108] Alternatively, by taking advantage of the high affinity of Hg^{2+} and Pb^{2+} toward Au NPs through the aurophilic interactions because of their similar electronic structures, a sensitive assay for the detection of the two analytes has been reported.[109] Once the analytes adsorb onto the surface of each Au NP, surface ligands are released to the bulk solution and induce aggregation of the Au NPs. Colorimetric visualization of Cu^{2+} has been demonstrated by taking its catalytic activity (Cu^{+}-catalyzed click chemistry) on the reaction of thiolated azide and alkyne functionalized Au NPs, with a LOD of 20 μM.[110] The functional Au NPs form aggregates after the reaction, mainly due to Cu^{+}-catalyzed cyclization of azide and alkyne. Similarly, azide and alkyne conjugated DNA modified Au NPs have also been applied to detect Cu^{2+} through Cu^{+}-induced crosslinking between adjacent DNA, with a LOD of 20 μM.[111] Although using DNA instead of a thiolate ligand to functionalize Au NPs is time-consuming, the resulting functional Au NPs provide high stability and reaction rate.

Disassembly mediated colorimetric sensing

Aggregation of Au NPs induces colloidal solution color changes from red to blue, while disassembly of aggregates leads to the reverse color variation. When compared to aggregation approaches, disassembly strategies show higher sensitivity due to the lower possibility of false positive signals. Several methods have been established for the colorimetric analysis of target analytes based on disassembly strategies.[112,113] A colorimetric Pb^{2+} sensing system was proposed based on DNAzyme-directed assembly of Au NPs, with a LOD of 100 nM.[114] The sensing system consists of DNA functionalized Au NPs, substrate ssDNA and DNAzyme. The substrate ssDNA contains complementary sequences in its head and tail ends to hybridize with the DNA on the surface of Au NPs, while its middle sequences hybridize DNAzyme. Mixing these three components leads to aggregation of Au NPs, leading to a blue solution color. The DNAzyme specifically interacts with Pb^{2+} to form a certain structure that catalyzes hydrolytic cleavage of substrate ssDNA, leading to disassembly of the Au NP aggregates and thus a solution color change to red after heating. This Pb^{2+} mediated detachment process can be accelerated (within 10 min) by adjusting the Au NPs size and distance between Au NPs.[115] The cleavage speed is greatly accelerated by replacing the small Au NPs (13 nm) with larger ones (42 nm) and extending the distance between Au NPs, mainly because of reduced steric hindrance and aggregate size. Similarly, the rate of disassembly is further accelerated by using a short length of DNA to hybridize with the cleaved substrate ssDNA fragments, which reduces the amount of free ssDNA fragments and promotes the cleavage of the substrate.[116,117]

An approach based on enzymatic disassembly of DNA–Au NP aggregates was developed for the colorimetric detection of the restriction endonuclease *Eco*RI.[118] DNA–Au NP aggregates were formed through the classical sandwich DNA structure that contains a recognition site for *Eco*RI. *Eco*RI induced cleavage of the rigid dsDNA, leading to disassembly of the Au NP aggregates into monodisperse Au NP and thus a corresponding shift in the absorption maximum from 534 to 524 nm. In addition to the determination of the activity of enzymes, a similar approach has been applied to quantitation of DNA, with a LOD of 200 nM.[119] To avoid the use of large size Au NP aggregates, dimers of aptamer functionalized Au NPs were prepared and used for sensing of microcystin-LR, a toxic peptide produced by cyanobacteria, with a LOD of 0.05 nM.[120] Upon the specific interaction of the aptamer with microcystin-LR, the dimers of aptamer functional Au NPs dissociate to form monomers. Having a smaller size of the dimer compared to conventional Au NP aggregates, this assay is complete within ~5 min, which is about 12 times faster than conventional approaches.

Analyte induced disassembly of aggregates of Au NPs functionalized with small ligands or polymers has also been reported.[121,122] A colorimetric system using piperazine–bisdithiocarbamate and citrate–Au NPs was developed for sensing of glutathione.[121] Bridge-linking coordination of piperazine–bisdithiocarbamate on the Au NP surface leads to aggregation of citrate–Au NPs. Through strong Au–S interactions between glutathione and Au NPs, surface replacement of the piperazinebisdithiocarbamate occurs, leading to disassembly of Au NP aggregates. Assembly of Au NPs through metal ion–ligand coordination can be disassembled after removal of the metal ions.[122,123] Aggregates of thiolated naphthalimide functionalized Au NPs induced by Hg^{2+} were used for screening of biothiols including glutathione, cysteine and homocysteine.[122] Addition of biothiols removes the Hg^{2+} and liberates individual Au NPs. The LODs of this approach for glutathione, cysteine and homocysteine are 17, 9 and 18 nM, respectively. To detect pyrophosphate anions, aggregates of thiolated dipycolylamine functionalized Au NPs induced by Mn^{2+} were used.[123] The assay provides different sensitivities for the three metal ions tested: $Mn^{2+} > Ni^{2+} > Cu^{2+}$, with a decreasing order that is in good agreement with their decreasing interaction strength with pyrophosphate anions.

Colorimetric assays on single Au NPs

Sensing systems based on the monitoring of the shift in the absorption wavelength have been applied for various analytes using functional Au NPs.[124,125] Monitoring of the formation of dimers of DNA functional Au NPs by dark field microscopy

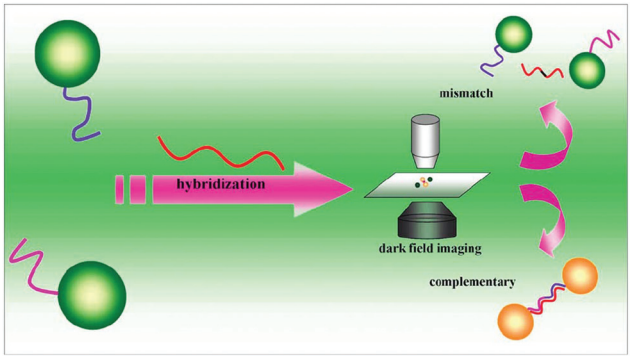

Fig. 4 DNA sandwich assay on single Au NPs. Reprinted with permission from ref. 126. Copyright 2010, American Chemical Society.

provided a LOD of 0.02 pM for target DNA, which is ~5 orders of magnitude lower than that obtained by conventional approaches.[126] Formation of the Au NP dimer results in interparticle coupling, leading a red-shift of scattering spectra and a color change that was observed using dark field microscopy (Fig. 4). By recording the number ratio of the dimer of Au NPs to the monodisperse Au NPs, the assay is sensitive for the detection of target DNA, with a LOD of 100 fM.[127] Quantitation of Cu^{2+} and monitoring of a click reaction were achieved by taking advantage of Cu^{+} catalyzing the formation of dimers of thiolated azide and alkyne functionalized Au NPs.[128] The simple assay provides a LOD of 0.1 nM for Cu^{2+}, based on the changes in the peak of scattering spectra of Au NPs. When using a laser instead of a white light source in a dark field microscopic system, a ~10 fold increase in the sensitivity for Hg^{2+} detection was achieved.[128]

The scattering color and absorption wavelength of single Au NPs can be altered by changing its morphology and/or size. For example, the catalytic deposition of Cu^{2+} on single Au NPs by the reduced nicotinamide adenine dinucleotide cofactor results in an increase of scattering maxima and a color change in dark field microscopy.[129] Such significant changes are mainly due to the change of the structure from sphere to core–shell after copper deposition onto the Au NPs. The assay holds potential for the study of reduced nicotinamide adenine dinucleotide dependent intracellular metabolic enzymatic pathways. To detect DNA, a single Au NP colorimetric system was developed based on the catalytic activity for the conversion of glucose and oxygen to form gluconic acid and hydrogen peroxide in the presence of glucose oxidase.[130] The as-formed hydrogen peroxide then catalyzes the decomposition of Au^{3+} on the surface of single Au NPs, leading to a gradual size enlargement of Au NPs and thus the scattering color change can be monitored with a dark field microscopic system. The catalytic activity of Au NPs is significantly inhibited by ssDNA that possesses strong binding affinity toward the Au NP surface. Adding complementary target DNA induces the formation of dsDNA, leading to the release of surface ssDNA and thus an increase in the catalytic activity of Au NPs. Similarly, single Au NP colorimetric systems were developed for the detection of dopamine based on dopamine mediated surface Au^{3+} decomposition, with a LOD of 0.25 pM,[131] and for the detection of Pb^{2+} based on Pb^{2+} accelerated Au NPs leaching in the presence of thiosulfate and 2-mercaptoethanol, with a LOD of 0.2 pM.[132]

Binding of small molecules to single Au NPs also causes the variation of the refractive index and changes in the scattering color of single Au NPs. By monitoring the changes in scattering light intensity of Au NP solutions, avidin was detected using biotin functionalized Au NPs, with a LOD of 1 nM.[133] The sensitivity can be further improved by using Au@Ag core–shell NPs as probes, mainly because of its greater extinction coefficient when compared to that of Au NPs. *In vivo* and *in vitro* H_2S detection was demonstrated using Au@Ag core–shell NPs, with LODs of 0.01 and 50 nM, respectively.[134,135] Through the interactions of H_2S with the surface Ag on the Au@Ag NPs, a Ag_2S shell was formed on each core of Au NP, resulting in a red-shift of scattering maxima and color changes in dark field microscopy. Alternatively, a technique based on imaging observation of color changes and counting of individual Au NPs through SPR microscopy was applied for sensitive detection of melamine and ATP, with LODs of 1 and 5 nM, respectively.[136]

Fluorescence detection

Au NP based fluorescence sensing systems have become more popular in analytical chemistry, mainly because of their sensitivity.[9,137,138] When compared to Au NP based colorimetric approaches, interference from the color sample matrix is minimized in the fluorescence system. The fluorescence approach also holds greater potential for cell imaging. Three kinds of Au NP based fluorescence sensing systems are discussed in this section: surface plasmon enhanced energy transfer, metal enhanced fluorescence and fluorescent Au NPs.

Surface plasmon enhanced energy transfer

Fluorescence resonance energy transfer (FRET) is an electrodynamic phenomenon that occurs between a donor fluorophore in the excited state and an acceptor fluorophore in the ground state. The donor molecules typically emit at shorter wavelengths that overlap with the absorption spectrum of the acceptor. The efficiency of FRET depends on several parameters, such as the spectral overlap of the emission spectrum of the donor with the absorption spectrum of the acceptor, the quantum yield of the donor, the relative orientation of the donor and acceptor transition dipoles, and the distance between the donor and acceptor molecules. Au NPs possess high extinction cross-section and surface electron density, which allows efficient energy transfer of fluorophores to their surface through dipole–surface interactions when they become close.[139] This so-called surface plasmon enhanced energy transfer (SPEET) has a higher efficiency than that of FRET, mainly because the isotropically distributed conducting electrons on the Au NP surface can interact strongly with the oscillating dipole of fluorophores.[140] Because dipole–surface rather than dipole–dipole interactions occur in SPEET, spectral

overlap between the emission spectrum of the donor and the absorption spectrum of Au NPs is not necessary.

Over the past few years, Au NP based SPEET systems have been extensively used for *in vitro* and *in vivo* detection of analytes of interest.[141,142] Compared with fluorescence turn-off approaches, target induced turn-on strategies have attracted growing interest because of their high sensitivity and low background. To achieve such a target induced fluorescence turn-on process, fluorophores are firstly adsorbed or immobilized on the Au NP surface to have maximum fluorescence quenching. The fluorescence recovers after the target interacts with the Au NPs/surface fluorophore as a result of increased distance between the fluorophore and the Au NP surface.[143,144] Higher sensitivity is usually achieved if the fluorophore molecules are released from the surface to the bulk solution. Rhodamine B absorbed Au NPs were used for the detection of Hg^{2+}.[145] Because Hg^{2+} has a strong affinity toward Au NPs, it interacts strongly with Au NP through d^{10}–d^{10} interactions, resulting in the release of rhodamine B from the surface to bulk solution and thus fluorescence restoration. This system allows selective Hg^{2+} detection over 50 fold that of other metal ions (*e.g.*, Pb^{2+}, Cd^{2+} and Co^{2+}), with a LOD of 10 nM. Similar approaches have been applied to sensing of various analytes such as thiolates, iodide anions, glyphosate and melamine.[146–149]

A protein sensing system using six cationic Au NPs and an anionic poly(*p*-phenylene ethynylene) fluorescent polymer was designed for the detection of seven proteins.[150] The electrostatic attraction between cationic Au NPs and the anionic polymer causes the fluorescence quenching of the fluorescent polymer. Proteins disrupt the Au NP–polymer complex *via* competitive binding and thus modulate the fluorescence quenching efficiency (Fig. 5). The fluorescence response pattern of individual proteins was characterized using linear discriminant analysis, providing a fingerprint for differentiation of seven proteins. Using the fluorophore conjugated DNA functionalized Au NP based sensing system, discrimination of eleven proteins was achieved.[151] DNA can be detected using Au NPs functionalized with fluorophore derivatized DNA having a hairpin structure.[152,153] In the hairpin structure on the Au NP surface, the fluorophore is close to the Au NP, leading to efficient fluorescence quenching. Once the constrained conformation changes in the presence of target DNA, the fluorophore is separated from Au NPs and the fluorescence is restored. A four-color nanobeacon sensing system using Au NPs conjugated with four different molecular beacons was developed for multiplexed detection and imaging of intracellular mRNAs (Fig. 6).[154] The four molecular beacons were derivatized with four different fluorophores. Hybridization between target mRNA and molecular beacons opens the hairpin structure and restores the fluorescence of the fluorophore. Different mRNAs generate unique fluorescence spectra (colors), which facilitate the discrimination of mRNA. This nanobeacon shows rapid response, high specificity, nuclease stability and good biocompatibility. With the assistance of a duplex-specific nuclease enzyme, quantification of as little as 0.2 fmol of miRNA-203 was achieved.[155] Direct quantification of cancer-related miRNA-203

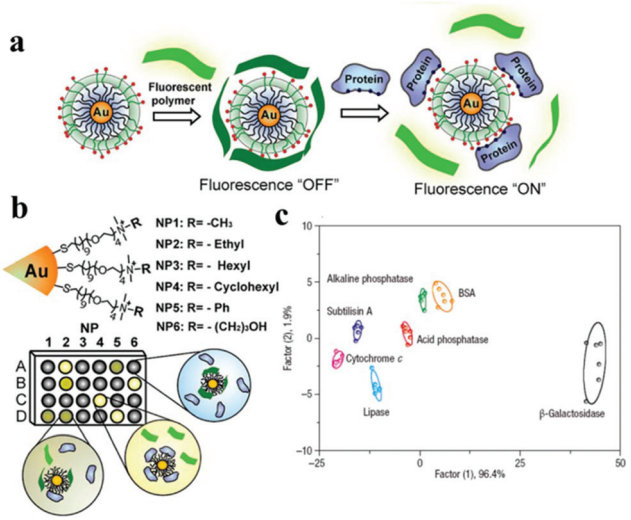

Fig. 5 Schematic depiction of the "chemical-nose" protein sensor array based on Au NP/fluorescent polymer conjugates. (a) Competitive binding between protein and Au NP–polymer induced fluorescence recovery. (b) The generation of fingerprint fluorescence response patterns with the combination of an array. (c) Canonical score plot for the first two factors of simplified response patterns of the Au NP–polymer array against proteins. Reprinted with permission from ref. 150. Copyright 2007, Nature Publishing Group.

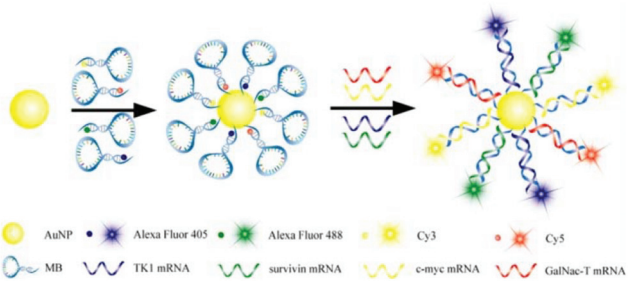

Fig. 6 Schematic diagram of multiple intracellular mRNA detection using four DNA–dye conjugate functionalized Au NP probes. Reprinted with permission from ref. 154. Copyright 2013, American Chemical Society.

and miRNA-21 in samples of extracted total RNA from cell cultures could be realized.

The fluorescence of fluorophores on the surface of Au NPs can be recovered by etching the Au core. Fluorescent polymer functionalized Au NP probes have been applied to sensing of cyanide, mainly because the cyanide anion is able to etch gold atoms to form $Au(CN)_2^-$ complexes.[156] Similarly, graphene oxide and amino pyrene-grafted Au NPs were used for the detection of Pb^{2+}.[157] In the absence of Pb^{2+}, the fluorescence of amino pyrene-grafted Au NPs is quenched by graphene oxide. Through the oxidation of Au NPs accelerated by Pb^{2+} in the presence of both thiosulfate and 2-mercaptoethanol, amino pyrene was released into aqueous solution and fluorescence was recovered.

Metal enhanced fluorescence

Au NPs can be used to enhance the fluorescence intensity of fluorophores that do not directly contact with Au NPs through the so-called metal enhanced fluorescence (MEF) effect.[158] SPR enhanced excitation and emission induced plasmon are responsible for the MEF effect.[159] The former causes an increase of the absorption cross-section of the fluorophore near the metal surface and subsequently an increase of fluorescence intensity. The latter results in an increase of induced plasmon scattering around the metal surface by partial energy from fluorophores and thus enhances the fluorescence intensity. In MEF, the proximity of the metal surface is necessary to ensure fluorescence enhancement. The optimal distance should be larger than ~11 nm to prevent the SPEET effect.[160,161] Fig. 7 shows the difference between SPEET and MEF. Since MEF is also based on the interaction between molecular dipole orientation and electric field around the metal surface, excitation wavelength and Au NP size show a magnificent influence on MEF efficiency.[162]

Using 100 nm of Au NPs as the substrate, MEF has been applied to the detection of DNA, with a LOD of 0.1 nM.[161] Upon DNA hybridization, the formation of duplex DNA makes fluorophores stay away from the Au NP surface, resulting in an increase of fluorescence. Several MEF approaches have been developed for enhanced sensitivity in the detection of various analytes such as levofloxacin (LOD, 0.2 nM), Hg^{2+} (LOD, 4.5 nM) and β-galactosidase (LOD, 100 nM).[163–165] Although MEF allows for improved sensitivity, the enhancement is usually limited to 10 fold.

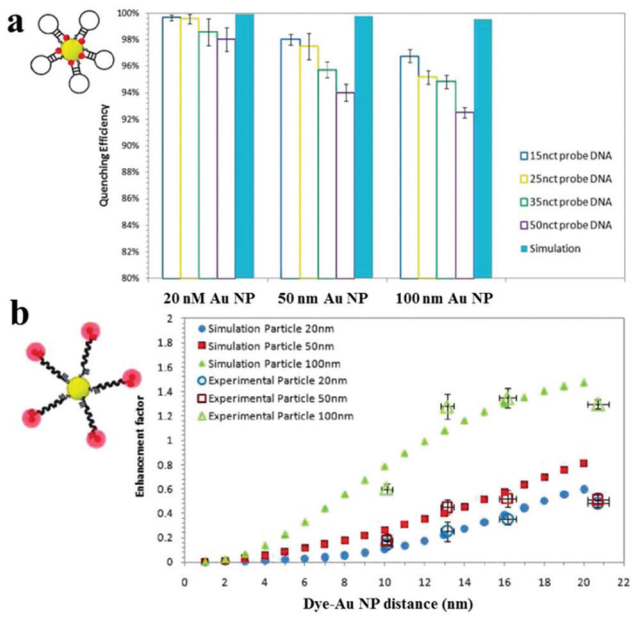

Fig. 7 Fluorescence quenching and enhancement by Au NP size and dye–Au NP distance. (a) Quenching efficiency as a function of Au NP size and DNA length. (b) Enhancement factor as a function of particle size and dye–Au NP distance. Reprinted with permission from ref. 161. Copyright 2011, American Chemical Society.

Fluorescent Au NPs

Some Au NPs with sizes smaller than 3 nm emit fluorescence, which are called gold nanoclusters (Au NCs) or gold nanodots (Au NDs).[26,166] They bridge the gap between individual atoms and large nanocrystals and display molecule-like properties. Because the size of fluorescent Au NPs is comparable to the Fermi wavelength of electrons, they show discrete electronic energy levels and unique physical and/or chemical properties different from large Au NPs. When compared with cadmium chalcogenide quantum dots and transition-metal-ion-doped quantum dots, fluorescent Au NPs show greater biocompatibility, but lower quantum yields.

It is believed that the fluorescence of fluorescent Au NPs originates from the correlation between metal centered electron transition and ligand–metal/metal–metal charge transfer.[167,168] Thus, the fluorescence of fluorescent Au NPs is primarily related to their size, structure, charge and surface ligand. Fig. 8 displays various colors of fluorescent Au NPs prepared using thiolates, polymers and biomolecules as ligands/scaffolds when excited with UV light.[169,170] Some review articles on fluorescent Au NPs have been published in the last three years,[21–23] thus only a brief discussion of their analytical applications is provided in this article. Most of the sensing methods using fluorescent Au NPs are based on a fluorescence turn-off strategy. Through the strong $5d^{10}$–$5d^{10}$ interaction between Hg^{2+} and Au^{+}, a sensitive and selective turn-off sensing system has been developed for the detection

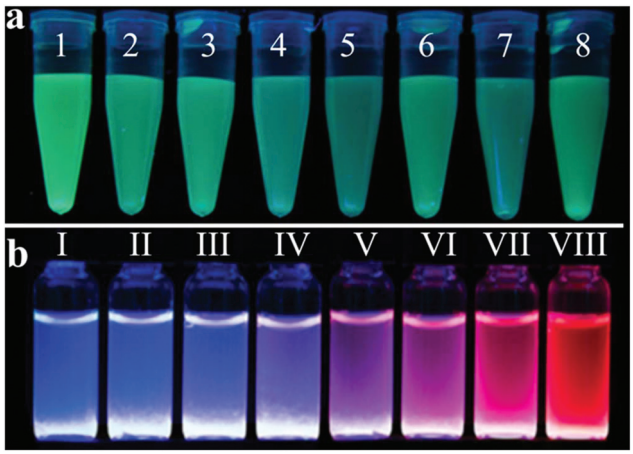

Fig. 8 Photographs of fluorescent Au NP solution under UV light illumination. (a) Dual-thiolate ligand cofunctionalized fluorescent Au NPs, from 1 to 8: GSH/MUA, TSH/MUA, MH/MUA, MPA/MUA, MSA/MUA, MEN/MUA, MBA/MUA, and NSH/MUA, respectively (MUA: 11-mercaptoundecanoic acid, GSH: glutathione, TSH: 1-(10-mercaptodecyl)-5-methylpyrimidine-2,4-dione), MH: 6-mercapto-1-hexanol, MPA: 3-mercaptopropionic acid, MSA: mercaptosuccinic acid, MEN: (2-mercaptoethyl)amine, MBA: 4-mercaptobenzoic acid, and NSH: (11-mercaptoundecyl)-*N*,*N*,*N*-trimethylammonium bromide). Reprinted with permission from ref. 169. Copyright 2015, American Chemical Society. (b) BSA protected fluorescent Au NPs containing Ce with different Ce/Au ratios, from I to VIII: 1000/0, 975/0.25, 950/0.5, 900/1.0, 800/2.0, 700/3.0, 500/5.0 and 0/10.0 μM/mM, respectively. Reprinted from ref. 170 with permission from the Royal Society of Chemistry.

of Hg^{2+}, with LOD at the nM level.[171] Fluorescence quenching through the surface ligand–analyte interaction has also been utilized for the detection of Pb^{2+}, Ag^{+}, H_2S or trinitrotoluene.[172–175] Bovine serum albumin (BSA) stabilized fluorescent Au NPs have been applied for the detection of thiolates and acetylcholinesterase through a surface ligand exchange strategy.[21,23] Both thiolate and protein stabilized fluorescent Au NPs have been used for the detection of hydrogen peroxide, with LODs of 27 and 30 nM, respectively.[176,177] The sensing mechanism is mainly based on the oxidation of Au atoms in the fluorescent Au NPs, leading to fluorescence quenching. Fluorescent Au NPs containing cerium (Ce) were used for intracellular pH monitoring based on a ratiometric approach.[170] The emission of the fluorescent Au NPs at 650 nm is insensitive to pH, while that for the BSA–Ce complex at 410 nm decreases with decreasing pH value. The fluorescent Au NPs containing Ce were further applied to sensing of CN^{-}, with a LOD of 50 nM.[178]

Fluorescent Au NPs have been used to detect biopolymers such as proteins, DNAs, cells and bacteria.[23,179,180] BSA templated fluorescent Au NPs have also been used to determine the activity/concentration of enzymes, such as trypsin, phosphatase and proteinase K, with LODs of 86, 210 and 5 pM, respectively.[181–183] The sensing mechanism is based on BSA degradation catalyzed by the enzymes, leading to fluorescence quenching. We note that the BSA template shell is very important to minimize fluorescence quenching by quenchers such as oxygen. Through different interactions of proteins with ligands on the surface of fluorescent Au NPs, fluorescent Au NPs conjugated with ligands such as proteins and thiolates have been used for the detection of proteins.[169,184,185] For example, dual-ligand cofunctionalized fluorescent Au NPs were used for the differentiation of eight proteins.[169] Using dual-ligand cofunctionalized fluorescent Au NP sensor arrays, eight proteins could be discriminated by analyzing the fluorescence response patterns *via* linear discriminant analysis. The protein induced fluorescence response of the fluorescent Au NPs is likely through the electrostatic as well as hydrophobic interactions between the surface thiolate ligands and protein amino acid residues.

SERS based sensing

Raman scattering is inelastic scattering of photons from a quantized vibrational signature. Both Raman shift and scattering intensity are sensitive to vibrational modes and provide feasibility for fingerprint sensing of target molecules. Unfortunately, direct use of Raman scattering for sensitive analyte detection is seriously restricted by the inherently weak Raman scattering intensity as a result of the small Raman scattering cross-section, which is 10–15 orders of magnitude smaller than that of fluorescence. The Raman scattering intensity can be enhanced dramatically (up to 14 orders of magnitude theoretically) by using plasmonic metal (*e.g.*, silver and gold) nanoparticles or films.[186,187] Such a physical phenomenon is called surface enhanced Raman scattering (SERS). Although the actual enhancement mechanism has not been completely understood, electromagnetic enhancement from LSPR/SPR and chemical enhancement through charge-transfer are generally accepted to be the two main contributions to SERS. The enhancement factor of SERS is related to the size, shape and surface properties of metal nanoparticles and also the interaction between the Raman reporter and metal nanoparticles.

Using Au NPs as substrates, sensitive detection of inorganic/organic ions, small molecules and biopolymers has been achieved by SERS.[188–193] For example, SERS was applied to the detection of CN^{-} by monitoring the SERS signal at 2154 cm^{-1} of $Au(CN)_2^{-}$ formed on the surface of Au NPs through etching of Au atoms by CN^{-}.[194] This approach provided a LOD of 100 ppt for CN^{-}. Using Raman dye conjugated DNA functionalized Au NPs, sensitive detection of Hg^{2+} was obtained, with a LOD of 0.1 nM.[195] Thymine–thymine mismatch in DNA templates hinders the formation of duplex DNA, which separates the Raman dye and Au NPs. In the presence of Hg^{2+}, thymine–Hg^{2+}–thymine coordination causes the hybridization of two DNA templates and promotes the formation of heterojunctions that can act as an excellent SERS platform.

SERS approaches using Au NPs have been applied to the detection of DNA.[196] Both DNA probes and Raman tags were functionalized onto the Au NP surface first, hybridization with target DNA results in the variation of Raman tags-Au NPs and thus change in the SERS intensity. To enhance the sensitivity of SERS for DNA, surface silver coating on Au NPs was prepared as a SERS promoter to generate strong SERS signals of Cy3 dye molecules.[197] This approach provided a LOD of 20 fM for target DNA. In conjunction with a chip device, this approach provided sensitive spectroscopic DNA fingerprinting for discrimination of six dissimilar DNA targets labeled with six Raman dyes. SERS approaches using Au NPs have also been demonstrated for the detection of proteins.[198,199] Pearl necklace Au nanomaterials (Au PNNs) showing high enhancement factor of Raman signals of rhodamine 6G up to 9 orders of magnitude has been reported.[199] Aptamer and 4-mercaptobenzoic acid (Raman reporter) functionalized Au NPs and Au PNNs (substrate) were used for sensitive detection of PDGF that is a potential marker of cancer diagnosis. The functionalized Au NPs first bind to PDGF through a specific aptamer–PDGF interaction, leading to purification and concentration of PDGF from the sample matrix as shown in Fig. 9. Then, PDGF containing Au NPs interact with Au PNNs through electrostatic attraction, and subsequently form aggregates with Au PNNs, leading to an enhanced Raman scattering signal of 4-mercaptobenzoic acid. Having a LOD of 0.5 pM for PDGF, this approach allowed quantitation of PDGF in urine samples.

The distance (gap) between adjacent Au NPs plays an important role in determining the magnitude of the SERS signal; the SERS signal increases as the gap decreases.[200,201] With ultrathin silica or alumina coating, shell-isolated Au NP probes provided enhanced SERS signals of pesticide residues.[200] The ultrathin coating prevents the Au NPs from aggregation, separates them from direct contact with the

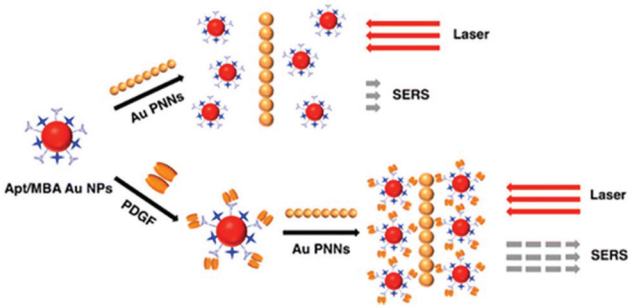

Fig. 9 Schematic representation of the Au PNNs based SERS assay for the sensing of PDGF protein. Reprinted with permission from ref. 199. Copyright 2014, American Chemical Society.

probed material and allows the Au NPs to conform to different contours of substrates. A tip coated with a monolayer of shell-isolated Au NPs provided SERS signal of Si–H stretching vibration with 2–3 orders of magnitude higher than that of an Au tip. This dramatic enhancement is attributed to the association of single shell-isolated Au NPs; each of them acts as an individual Au tip. Alternatively, methoxy-mercaptopoly (ethylene glycol) was used to conjugate Au NPs to form dense monolayer films with 5 nm gaps, which provides a large SERS enhancement with an enhancement factor of $\sim 10^7$.[202] The gap between adjacent Au NPs can also be controlled by the modification of the surface of each Au NP with DNA. Compared to bare Au NPs, DNA–Au NPs as a substrate yield higher SERS signals for the tested analytes, including rhodamine 6G, trinitrotoluene and 4-aminothiophenol, leading to at least one order of magnitude lower LODs.[203] When the gap between DNA–Au NP was shortened to 1–3 nm, SERS signals of 4-aminothiophenol with enhancement factors up to $\sim 10^9$ were achieved.[204] Such a high SERS active substrate provided sensitive 4-aminothiophenol detection with a LOD of 0.5 nM.

Because the enhancement factor of shell-isolated Au NPs is largely dependent on its core size and shell thickness,[205] SERS signals of analytes can be further controlled by varying the sizes of the core and the shell of shell-isolated Au NPs. More importantly, the chemically inert shell avoids direct contact between the adsorbates and bare Au NPs, which allows observation of the true vibrational information of probed materials. Thus, the shell-isolated Au NP substrates provide more unfeigned Raman signal when compared to that of bare Au NP substrates. The shell-isolated Au NP substrates have been shown to be powerful for the analyses of cell walls and single molecules, food inspection, and monitoring of adsorption processes.[206–208]

Conclusion and outlooks

In this review, we have presented an overview of the progress of absorption, fluorescence and SERS-based optical sensing systems using Au NP probes. Most of these Au NP probes show enhanced sensitivity and selectivity toward chemical and biological agents, based on analyte induced changes in absorbance, fluorescence or Raman signals. These sensing systems are dependent on the analyte induced changes in the size or morphology of Au NPs or the distance between Au NPs. Most of the sensing systems provide LOD at the nM level for tested analytes. With signal amplification or special detection systems, some Au NP based optical systems allow detection of analytes down to pM and even fM levels.

Although many Au NP based optical systems have been shown to be practical for the analysis of various samples, most reported systems can only be applied for the analysis of samples with low interference and ionic strength. Matrix and salt effects are still problematic for most developed sensing systems. False results occur commonly as a result of serious matrix interference. For the analysis of complicated samples, sample dilution and preconcentration of analytes are needed. They may however suffer from the change in the species of analytes, loss of the sample, contamination, and/or being time consuming. It is extremely difficult to achieve quantitation of trace amounts of analytes such as proteins in blood samples containing abundant proteins. For example, aptamer functionalized Au NPs cannot be applied to quantitation of PDGF in blood samples without sample pretreatment. Many signal amplification strategies applied in Au NP based sensing systems are time consuming or require the use of expensive enzymes. Special detection systems such as those used for monitoring single Au NPs require operators with a special skill.

Although single Au NP based approaches provide higher sensitivity than traditional Au NP based ones, sophisticated optical systems and Au NPs with a very narrow size distribution are needed. Thus, low-cost and automatic optical systems such as high-throughput microarrays and droplet-based microfluidics are in demand. Strategies such as using mild reducing agents with stronger capping strength than citrate for preparation of Au NPs with a narrow size distribution are worth trying. Cofunctionalization of Au NPs with ligands having different chemical/physical/recognition properties can be used to further improve the selectivity of the analyte, with minimum matrix interference. Functional magnetic nanoparticles have been shown to be effective for removal of the matrix and concentration of trace analytes before applying Au NPs for detection.[209,210] However, the process is usually tedious and requires large sample volumes. It would be more effective if multifunctional Au NP composites can be prepared. For example, most of the matrix and salt are excluded by the shell and only analytes can interact with Au NPs inside the composites, leading to signal changes. It is also interesting to design Au NPs having enzyme-like properties and interesting optical properties as a new type of sensing system with enhanced selectivity and sensitivity.[211–213] To speed up signal amplification, micro analysis systems in conjunction with Au NP based systems are a possible solution. Multichannel detection approaches (*i.e.*, absorption/fluorescence, absorption/Raman or fluorescence/Raman) will be useful to further

improve their reliability and practicability for the analysis of complicated biological and environmental samples.

Acknowledgements

This work was supported by the Ministry of Science and Technology of Taiwan under contracts NSC 104-2113-M-002-008-MY3 and 103-2923-M-002-002-MY3. This work was also supported by the National Basic Research Program of China (973 Program, 2014CB932103) and the National Natural Foundation of China (21375006 and 21575010), and the Free Exploration Project of Beijing University of Chemical Technology (ZY1625).

Notes and references

1 H. Kobayashi, M. Ogawa, R. Alford, P. L. Choyke and Y. Urano, *Chem. Rev.*, 2010, **110**, 2620.
2 H. Ma, J. Liu, M. M. Ali, M. A. I. Mahmood, L. Labanieh, M. Lu, S. M. Iqbal, Q. Zhang, W. Zhao and Y. Wan, *Chem. Soc. Rev.*, 2015, **44**, 1240.
3 S. Song, Y. Qin, Y. He, Q. Huang, C. Fan and H.-Y. Chen, *Chem. Soc. Rev.*, 2010, **39**, 4234.
4 Y. Song, W. Wei and X. Qu, *Adv. Mater.*, 2011, **23**, 4215.
5 M. Grzelczak, J. Perez-Juste, P. Mulvaney and L. M. Liz-Marzan, *Chem. Soc. Rev.*, 2008, **37**, 1783.
6 Y.-W. Lin, C.-C. Huang and H.-T. Chang, *Analyst*, 2011, **136**, 863.
7 H. Jans and Q. Huo, *Chem. Soc. Rev.*, 2012, **41**, 2849.
8 Y. Sun and Y. Xia, *Analyst*, 2003, **128**, 686.
9 A. Heuer-Jungemann, P. K. Harimech, T. Brown and A. G. Kanaras, *Nanoscale*, 2013, **5**, 9503.
10 V. K. K. Upadhyayula, *Anal. Chim. Acta*, 2012, **715**, 1.
11 X. Yang, M. Yang, B. Pang, M. Vara and Y. Xia, *Chem. Rev.*, 2015, **115**, 10410.
12 W. Zhou, X. Gao, D. Liu and X. Chen, *Chem. Rev.*, 2015, **115**, 10575.
13 M. Li, S. K. Cushing and N. Wu, *Analyst*, 2015, **140**, 386.
14 K. Saha, S. S. Agasti, C. Kim, X. Li and V. M. Rotello, *Chem. Rev.*, 2012, **112**, 2739.
15 W. Zhao, M. A. Brook and Y. Li, *ChemBioChem*, 2008, **9**, 2363.
16 P. Zhao, N. Li and D. Astruc, *Coord. Chem. Rev.*, 2013, **257**, 638.
17 T. Jain, Q. Tang, T. Bjørnholm and K. Nørgaard, *Acc. Chem. Res.*, 2014, **47**, 2.
18 J. Turkevich, P. C. Stevenson and J. Hillier, *Discuss. Faraday Soc.*, 1951, **11**, 55.
19 G. Frens, *Nat. Phys. Sci.*, 1973, **241**, 20.
20 M. Brust, M. Walker, D. Bethell, D. J. Schiffrin and R. Whyman, *J. Chem. Soc., Chem. Commun.*, 1994, 801.
21 Z. Luo, K. Zheng and J. Xie, *Chem. Commun.*, 2014, **50**, 5143.
22 Y. Tao, M. Li, J. Ren and X. Qu, *Chem. Soc. Rev.*, 2015, **44**, 8636.
23 L.-Y. Chen, C.-W. Wang, Z. Yuan and H.-T. Chang, *Anal. Chem.*, 2015, **87**, 216.
24 X. Su, H. Jiang and X. Wang, *Anal. Chem.*, 2015, **87**, 10230.
25 Y. Yu, Z. Luo, D. M. Chevrier, D. T. Leong, P. Zhang, D.-E. Jiang and J. Xie, *J. Am. Chem. Soc.*, 2014, **136**, 1246.
26 C.-C. Huang, Z. Yang, K.-H. Lee and H.-T. Chang, *Angew. Chem., Int. Ed.*, 2007, **46**, 6824.
27 Y.-T. Tseng, Z. Yuan, Y.-Y. Yang, C.-C. Huang and H.-T. Chang, *RSC Adv.*, 2014, **4**, 33629–33635.
28 K. M. Mayer and J. H. Hafner, *Chem. Rev.*, 2011, **111**, 3828.
29 H. Du, R.-C. A. Fuh, J. Li, L. A. Corkan and J. S. Lindsey, *Photochem. Photobiol.*, 1998, **68**, 141.
30 W. Haiss, N. T. K. Thanh, J. Aveyard and D. G. Fernig, *Anal. Chem.*, 2007, **79**, 4215.
31 G. Mie, *Ann. Phys.*, 1908, **330**, 377.
32 R. Elghanian, J. J. Storhoff, R. C. Mucic, R. L. Letsinger and C. A. Mirkin, *Science*, 1997, **277**, 1078.
33 Z. Yuan, J. Cheng, X. Cheng, Y. He and E. S. Yeung, *Analyst*, 2012, **137**, 2930.
34 H. Yin, X. Huang, W. Ma, L. Xu, S. Zhu, H. Kuang and C. Xu, *Biosens. Bioelectron.*, 2014, **52**, 8.
35 E. Nourisaeid, A. Mousavi and A. Arpanaei, *Physica E*, 2016, **75**, 188.
36 M. Mancuso, L. Jiang, E. Cesarman and D. Erickson, *Nanoscale*, 2013, **5**, 1678.
37 K. Kalidasan, J. L. Neo and M. Uttamchandani, *Mol. BioSyst.*, 2013, **9**, 618.
38 O. Doluca, J. M. Withers and V. V. Filichev, *Chem. Rev.*, 2013, **113**, 3044.
39 C. Xiong, C. Wu, H. Zhang and L. Ling, *Spectrochim. Acta, Part A*, 2011, **79**, 956.
40 Z. Chen, H. Zhang, X. Ma, Z. Lin, L. Zhang and G. Chen, *Analyst*, 2015, **140**, 7742.
41 A. K. R. Lytton-Jean, M. S. Han and C. A. Mirkin, *Anal. Chem.*, 2007, **79**, 6037.
42 G. Wang, Y. Akiyama, T. Takarada and M. Maeda, *Chem. – Eur. J.*, 2016, **22**, 258.
43 P. Valentini and P. P. Pompa, *RSC Adv.*, 2013, **3**, 19181.
44 J. Liu, *Phys. Chem. Chem. Phys.*, 2012, **14**, 10485.
45 K. M. Koo, A. A. I. Sina, L. G. Carrascosa, M. J. A. Shiddiky and M. Trau, *Anal. Methods*, 2015, **7**, 7042.
46 H. Li and L. J. Rothberg, *J. Am. Chem. Soc.*, 2004, **126**, 10958.
47 X. Zhang, M. R. Servos and J. Liu, *Langmuir*, 2012, **28**, 3896.
48 X. Zhang, M. R. Servos and J. Liu, *J. Am. Chem. Soc.*, 2012, **134**, 7266.
49 X. Zhang, T. Gouriye, K. Göeken, M. R. Servos, R. Gill and J. Liu, *J. Phys. Chem. C*, 2013, **117**, 15677.
50 P. Liu, X. Yang, S. Sun, Q. Wang, K. Wang, J. Huang, J. Liu and L. He, *Anal. Chem.*, 2013, **85**, 7689.
51 H. Deng, X. Zhang, A. Kumar, G. Zou, X. Zhang and X.-J. Liang, *Chem. Commun.*, 2013, **49**, 51.
52 S. Abdul Rahman, R. Saadun, N. E. Azmi, N. Ariffin, J. Abdullah, N. A. Yusof, H. Sidek and R. Hajian, *J. Nanomater.*, 2014, **2014**, 5.

53 V. G. Joshi, K. Chindera, A. K. Singh, A. P. Sahoo, V. D. Dighe, D. Thakuria, A. K. Tiwari and S. Kumar, *Anal. Chim. Acta*, 2013, **795**, 1.
54 H. Deng, Y. Xu, Y. Liu, Z. Che, H. Guo, S. Shan, Y. Sun, X. Liu, K. Huang, X. Ma, Y. Wu and X.-J. Liang, *Anal. Chem.*, 2012, **84**, 1253.
55 J. Gao, L. Ma, Z. Lei and Z. Wang, *Analyst*, 2016, DOI: 10.1039/C5AN02510A.
56 L. Guo, Y. Xu, A. R. Ferhan, G. Chen and D.-H. Kim, *J. Am. Chem. Soc.*, 2013, **135**, 12338.
57 M. B. Pepys, G. M. Hirschfield, G. A. Tennent, J. Ruth Gallimore, M. C. Kahan, V. Bellotti, P. N. Hawkins, R. M. Myers, M. D. Smith, A. Polara, A. J. A. Cobb, S. V. Ley, J. Andrew Aquilina, C. V. Robinson, I. Sharif, G. A. Gray, C. A. Sabin, M. C. Jenvey, S. E. Kolstoe, D. Thompson and S. P. Wood, *Nature*, 2006, **440**, 1217.
58 G. He, W. Luo, P. Li, C. Remmers, W. J. Netzer, J. Hendrick, K. Bettayeb, M. Flajolet, F. Gorelick, L. P. Wennogle and P. Greengard, *Nature*, 2010, **467**, 95.
59 S. Sun, H. Shen, C. Liu and Z. Li, *Analyst*, 2015, **140**, 5685.
60 Y. T. Ho, B. Poinard, E. L. L. Yeo and J. C. Y. Kah, *Analyst*, 2015, **140**, 1026.
61 Y. Zhu, G. Wang, L. Sha, Y. Qiu, H. Jiang and X. Zhang, *Analyst*, 2015, **140**, 1260.
62 C. L. Schofield, B. Mukhopadhyay, S. M. Hardy, M. B. McDonnell, R. A. Field and D. A. Russell, *Analyst*, 2008, **133**, 626.
63 L. Otten, S.-J. Richards, E. Fullam, G. S. Besra and M. I. Gibson, *J. Mater. Chem. B*, 2013, **1**, 2665.
64 K. Aslan, C. C. Luhrs and V. H. Pérez-Luna, *J. Phys. Chem. B*, 2004, **108**, 15631.
65 P. Chen, M. T. Chung, W. McHugh, R. Nidetz, Y. Li, J. Fu, T. T. Cornell, T. P. Shanley and K. Kurabayashi, *ACS Nano*, 2015, **9**, 4173.
66 M. Bhagawati, C. You and J. Piehler, *Anal. Chem.*, 2013, **85**, 9564.
67 W.-J. Kim, H. Y. Cho, B. K. Kim, C. Huh, K. H. Chung, C.-G. Ahn, Y. J. Kim and A. Kim, *Sens. Actuators, B*, 2015, **221**, 537.
68 X. Huang, Z. Xu, Y. Mao, Y. Ji, H. Xu, Y. Xiong and Y. Li, *Biosens. Bioelectron.*, 2015, **66**, 184.
69 Q. He, Z. Zhu, L. Jin, L. Peng, W. Guo and S. Hu, *J. Anal. At. Spectrom.*, 2014, **29**, 1477.
70 C.-C. Huang, Y.-F. Huang, Z. Cao, W. Tan and H.-T. Chang, *Anal. Chem.*, 2005, **77**, 5735.
71 T.-E. Lin, W.-H. Chen, Y.-C. Shiang, C.-C. Huang and H.-T. Chang, *Biosens. Bioelectron.*, 2011, **29**, 204.
72 C.-K. Chen, C.-C. Huang and H.-T. Chang, *Biosens. Bioelectron.*, 2010, **25**, 1922.
73 R. Selegard, K. Enander and D. Aili, *Nanoscale*, 2014, **6**, 14204.
74 D. Huang, C. Niu, Z. Li, M. Ruan, X. Wang and G. Zeng, *Analyst*, 2012, **137**, 5607.
75 W. Xue, G. Zhang and D. Zhang, *Analyst*, 2011, **136**, 3136.
76 L. Zhang, J. Zhao, J. Jiang and R. Yu, *Chem. Commun.*, 2012, **48**, 10996.
77 F. Cheng, Y. He, X.-J. Xing, D.-D. Tan, Y. Lin, D.-W. Pang and H.-W. Tang, *Analyst*, 2015, **140**, 1572.
78 E. Hutter and D. Maysinger, *Trends Pharmacol. Sci.*, 2013, **34**, 497.
79 D. Liu, Z. Wang, A. Jin, X. Huang, X. Sun, F. Wang, Q. Yan, S. Ge, N. Xia, G. Niu, G. Liu, A. R. Hight Walker and X. Chen, *Angew. Chem., Int. Ed.*, 2013, **52**, 14065.
80 J.-H. Lin, C.-W. Chang, Z.-H. Wu and W.-L. Tseng, *Anal. Chem.*, 2010, **82**, 8775.
81 L.-J. Ou, P.-Y. Jin, X. Chu, J.-H. Jiang and R.-Q. Yu, *Anal. Chem.*, 2010, **82**, 6015.
82 S. Bi, X. Jia, J. Ye and Y. Dong, *Biosens. Bioelectron.*, 2015, **71**, 427.
83 J. Zhang, X. Xu and X. Yang, *Analyst*, 2012, **137**, 1556.
84 Z. Chen, Z. Wang, J. Chen, S. Wang and X. Huang, *Analyst*, 2012, **137**, 3132.
85 J. Zhang, X. Wang and X. Yang, *Analyst*, 2012, **137**, 2806.
86 Y. Jiang, H. Zhao, N. Zhu, Y. Lin, P. Yu and L. Mao, *Angew. Chem., Int. Ed.*, 2008, **47**, 8601.
87 X. Liang, H. Wei, Z. Cui, J. Deng, Z. Zhang, X. You and X.-E. Zhang, *Analyst*, 2011, **136**, 179.
88 F. Wang, X. Liu, C.-H. Lu and I. Willner, *ACS Nano*, 2013, **7**, 7278.
89 Y.-Y. Yu, L. Zhang, X.-Y. Sun, C.-L. Li, Y. Qiu, H.-P. Sun, D.-Q. Tang, Y.-W. Liu and X.-X. Yin, *Chem. Commun.*, 2015, **51**, 8880.
90 J. Peng, Y. Wang, L. Liu, H. Kuang, A. Li and C. Xu, *RSC Adv.*, 2016, **6**, 7798.
91 S. Cheng, B. Zheng, M. Wang, M. H.-W. Lam and X. Ge, *Talanta*, 2013, **115**, 506.
92 F. Li, J. Zhang, X. Cao, L. Wang, D. Li, S. Song, B. Ye and C. Fan, *Analyst*, 2009, **134**, 1355.
93 S.-J. Chen, Y.-F. Huang, C.-C. Huang, K.-H. Lee, Z.-H. Lin and H.-T. Chang, *Biosens. Bioelectron.*, 2008, **23**, 1749.
94 J. Hu, P. Ni, H. Dai, Y. Sun, Y. Wang, S. Jiang and Z. Li, *Analyst*, 2015, **140**, 3581.
95 J. Liu, W. Bai, S. Niu, C. Zhu, S. Yang and A. Chen, *Sci. Rep.*, 2014, **4**, 7571.
96 J. Xu, Y. Li, J. Bie, W. Jiang, J. Guo, Y. Luo, F. Shen and C. Sun, *Microchim. Acta*, 2015, **182**, 2131.
97 M. Hoang, P.-J. J. Huang and J. Liu, *ACS Sens.*, 2016, DOI: 10.1021/acssensors.5b00147.
98 D. Kato and M. Oishi, *ACS Nano*, 2014, **8**, 9988.
99 J. Zhang, Y. Liu, J. Lv and G. Li, *Nano Res.*, 2015, **8**, 920.
100 B. Kong, A. Zhu, Y. Luo, Y. Tian, Y. Yu and G. Shi, *Angew. Chem., Int. Ed.*, 2011, **50**, 1837.
101 Z. Yuan, F. Lu, M. Peng, C.-W. Wang, Y.-T. Tseng, Y. Du, N. Cai, C.-W. Lien, H.-T. Chang, Y. He and E. S. Yeung, *Anal. Chem.*, 2015, **87**, 7267.
102 W. Chansuvarn, T. Tuntulani and A. Imyim, *Trends Anal. Chem.*, 2015, **65**, 83.
103 J.-S. Lee, M. S. Han and C. A. Mirkin, *Angew. Chem., Int. Ed.*, 2007, **46**, 4093.
104 G.-H. Chen, W.-Y. Chen, Y.-C. Yen, C.-W. Wang, H.-T. Chang and C.-F. Chen, *Anal. Chem.*, 2014, **86**, 6843.
105 G. Sener, L. Uzun and A. Denizli, *Anal. Chem.*, 2014, **86**, 514.

106 Y. Ma, L. Jiang, Y. Mei, R. Song, D. Tian and H. Huang, *Analyst*, 2013, **138**, 5338.
107 F. Chai, C. Wang, T. Wang, L. Li and Z. Su, *ACS Appl. Mater. Interfaces*, 2010, **2**, 1466.
108 L. Li, Z. Yuan, X. Peng, L. Li, J. He and Y. Zhang, *J. Chin. Chem. Soc.*, 2014, **61**, 1371.
109 Y.-R. Kim, R. K. Mahajan, J. S. Kim and H. Kim, *ACS Appl. Mater. Interfaces*, 2010, **2**, 292.
110 Y. Zhou, S. Wang, K. Zhang and X. Jiang, *Angew. Chem., Int. Ed.*, 2008, **47**, 7454.
111 X. Xu, W. L. Daniel, W. Wei and C. A. Mirkin, *Small*, 2010, **6**, 623.
112 X. Han, Y. Liu and Y. Yin, *Nano Lett.*, 2014, **14**, 2466.
113 M. Zhang, G. Qing, C. Xiong, R. Cui, D.-W. Pang and T. Sun, *Adv. Mater.*, 2013, **25**, 749.
114 J. Liu and Y. Lu, *J. Am. Chem. Soc.*, 2003, **125**, 6642.
115 J. Liu and Y. Lu, *J. Am. Chem. Soc.*, 2004, **126**, 12298.
116 J. Liu and Y. Lu, *J. Am. Chem. Soc.*, 2005, **127**, 12677.
117 J. H. Lee, Z. Wang, J. Liu and Y. Lu, *J. Am. Chem. Soc.*, 2008, **130**, 14217.
118 A. G. Kanaras, Z. Wang, M. Brust, R. Cosstick and A. D. Bates, *Small*, 2007, **3**, 590.
119 I. A. Trantakis, S. Bolisetty, R. Mezzenga and S. J. Sturla, *Langmuir*, 2013, **29**, 10824.
120 F. Wang, S. Liu, M. Lin, X. Chen, S. Lin, X. Du, H. Li, H. Ye, B. Qiu, Z. Lin, L. Guo and G. Chen, *Biosens. Bioelectron.*, 2015, **68**, 475.
121 Y. Li, P. Wu, H. Xu, H. Zhang and X. Zhong, *Analyst*, 2011, **136**, 196.
122 H. Xu, Y. Wang, X. Huang, Y. Li, H. Zhang and X. Zhong, *Analyst*, 2012, **137**, 924.
123 D. X. Li, J. F. Zhang, Y. H. Jang, Y. J. Jang, D. H. Kim and J. S. Kim, *Small*, 2012, **8**, 1442.
124 L. Xiao and E. S. Yeung, *Annu. Rev. Anal. Chem.*, 2014, **7**, 89.
125 Y. Peng, B. Xiong, L. Peng, H. Li, Y. He and E. S. Yeung, *Anal. Chem.*, 2015, **87**, 200.
126 L. Xiao, L. Wei, Y. He and E. S. Yeung, *Anal. Chem.*, 2010, **82**, 6308.
127 T. Bu, T. Zako, M. Fujita and M. Maeda, *Chem. Commun.*, 2013, **49**, 7531.
128 X. Cheng, D. Dai, Z. Yuan, L. Peng, Y. He and E. S. Yeung, *Anal. Chem.*, 2014, **86**, 7584.
129 L. Zhang, Y. Li, D.-W. Li, C. Jing, X. Chen, M. Lv, Q. Huang, Y.-T. Long and I. Willner, *Angew. Chem., Int. Ed.*, 2011, **50**, 6789.
130 X. Zheng, Q. Liu, C. Jing, Y. Li, D. Li, W. Luo, Y. Wen, Y. He, Q. Huang, Y.-T. Long and C. Fan, *Angew. Chem., Int. Ed.*, 2011, **50**, 11994.
131 W. W. Qin, S. P. Wang, J. Li, T. H. Peng, Y. Xu, K. Wang, J. Y. Shi, C. H. Fan and D. Li, *Nanoscale*, 2015, **7**, 15070.
132 D. Dai, D. Xu, X. Cheng and Y. He, *Anal. Methods*, 2014, **6**, 4507.
133 Y. Liu and C. Z. Huang, *Chem. Commun.*, 2013, **49**, 8262.
134 B. Xiong, R. Zhou, J. Hao, Y. Jia, Y. He and E. S. Yeung, *Nat. Commun.*, 2013, **4**, 1708.
135 J. Hao, B. Xiong, X. Cheng, Y. He and E. S. Yeung, *Anal. Chem.*, 2014, **86**, 4663.
136 L. Yuan, X. Wang, Y. Fang, C. Liu, D. Jiang, X. Wo, W. Wang and H.-Y. Chen, *Anal. Chem.*, 2016, DOI: 10.1021/acs.analchem.5b04244.
137 D. Liu, Z. Wang and X. Jiang, *Nanoscale*, 2011, **3**, 1421.
138 D. Ghosh and N. Chattopadhyay, *J. Lumin.*, 2015, **160**, 223.
139 P. C. Ray, Z. Fan, R. A. Crouch, S. S. Sinha and A. Pramanik, *Chem. Soc. Rev.*, 2014, **43**, 6370.
140 C. S. Yun, A. Javier, T. Jennings, M. Fisher, S. Hira, S. Peterson, B. Hopkins, N. O. Reich and G. F. Strouse, *J. Am. Chem. Soc.*, 2005, **127**, 3115.
141 D. Huang, C. Niu, X. Wang, X. Lv and G. Zeng, *Anal. Chem.*, 2013, **85**, 1164.
142 J.-M. Liu, J.-T. Chen and X.-P. Yan, *Anal. Chem.*, 2013, **85**, 3238.
143 L. Li, J. Feng, Y. Fan and B. Tang, *Anal. Chem.*, 2015, **87**, 4829.
144 Z. Wu, G.-Q. Liu, X.-L. Yang and J.-H. Jiang, *J. Am. Chem. Soc.*, 2015, **137**, 6829.
145 C.-C. Huang and H.-T. Chang, *Anal. Chem.*, 2006, **78**, 8332.
146 J. Xu, H. Yu, Y. Hu, M. Chen and S. Shao, *Biosens. Bioelectron.*, 2016, **75**, 1.
147 W. Li, Y. Dong, X. Wang, H. Li and D. Xu, *Biosens. Bioelectron.*, 2015, **66**, 43.
148 J. Guo, Y. Zhang, Y. Luo, F. Shen and C. Sun, *Talanta*, 2014, **125**, 385.
149 X. Cao, F. Shen, M. Zhang, J. Guo, Y. Luo, X. Li, H. Liu, C. Sun and J. Liu, *Food Control*, 2013, **34**, 221.
150 C. C. You, O. R. Miranda, B. Gider, P. S. Ghosh, I. B. Kim, B. Erdogan, S. A. Krovi, U. H. Bunz and V. M. Rotello, *Nat. Nanotechnol.*, 2007, **2**, 31.
151 W. Sun, Y. Lu, J. Mao, N. Chang, J. Yang and Y. Liu, *Anal. Chem.*, 2015, **87**, 3354.
152 J. Xue, L. Shan, H. Chen, Y. Li, H. Zhu, D. Deng, Z. Qian, S. Achilefu and Y. Gu, *Biosens. Bioelectron.*, 2013, **41**, 71.
153 A. Giannetti, S. Tombelli and F. Baldini, *Anal. Bioanal. Chem.*, 2013, **405**, 6181.
154 W. Pan, T. Zhang, H. Yang, W. Diao, N. Li and B. Tang, *Anal. Chem.*, 2013, **85**, 10581.
155 F. Degliangeli, P. Kshirsagar, V. Brunetti, P. P. Pompa and R. Fiammengo, *J. Am. Chem. Soc.*, 2014, **136**, 2264.
156 L. Shang, L. Zhang and S. Dong, *Analyst*, 2009, **134**, 107.
157 X. Shi, W. Gu, W. Peng, B. Li, N. Chen, K. Zhao and Y. Xian, *ACS Appl. Mater. Interfaces*, 2014, **6**, 2568.
158 J. R. Lakowicz, B. Shen, Z. Gryczynski, S. D'Auria and I. Gryczynski, *Biochem. Biophys. Res. Commun.*, 2001, **286**, 875.
159 J. Lakowicz, *Plasmonics*, 2006, **1**, 5.
160 J. Zhang and J. R. Lakowicz, *Opt. Express*, 2007, **15**, 2598.
161 Y. Cheng, T. Stakenborg, P. Van Dorpe, L. Lagae, M. Wang, H. Chen and G. Borghs, *Anal. Chem.*, 2011, **83**, 1307.
162 M. Li, Q. Wang, X. Shi, L. A. Hornak and N. Wu, *Anal. Chem.*, 2011, **83**, 7061.

163 S. H. Lee, S. M. Wabaidur, Z. A. Alothman and S. M. Alam, *Luminescence*, 2011, **26**, 768.
164 Z. Cheng, G. Li and M. Liu, *Sens. Actuators, B*, 2015, **212**, 495.
165 Z. Zeng, S. Mizukami, K. Fujita and K. Kikuchi, *Chem. Sci.*, 2015, **6**, 4934.
166 J. Zheng, P. R. Nicovich and R. M. Dickson, *Annu. Rev. Phys. Chem.*, 2007, **58**, 409.
167 J. Zheng, C. Zhou, M. Yu and J. Liu, *Nanoscale*, 2012, **4**, 4073.
168 J. Zheng, C. Zhang and R. M. Dickson, *Phys. Rev. Lett.*, 2004, **93**, 077402.
169 Z. Yuan, Y. Du, Y.-T. Tseng, M. Peng, N. Cai, Y. He, H.-T. Chang and E. S. Yeung, *Anal. Chem.*, 2015, **87**, 4253.
170 Y.-N. Chen, P.-C. Chen, C.-W. Wang, Y.-S. Lin, C.-M. Ou, L.-C. Ho and H.-T. Chang, *Chem. Commun.*, 2014, **50**, 8571.
171 J. Xie, Y. Zheng and J. Y. Ying, *Chem. Commun.*, 2010, **46**, 961.
172 Z. Yuan, M. Peng, Y. He and E. S. Yeung, *Chem. Commun.*, 2011, **47**, 11981.
173 P.-C. Chen, T.-Y. Yeh, C.-M. Ou, C.-C. Shih and H.-T. Chang, *Nanoscale*, 2013, **5**, 4691.
174 A. Senthamizhan, A. Celebioglu and T. Uyar, *Chem. Commun.*, 2015, **51**, 5590.
175 Z. Yuan, M. Peng, L. Shi, Y. Du, N. Cai, Y. He, H.-T. Chang and E. S. Yeung, *Nanoscale*, 2013, **5**, 4683.
176 H.-H. Deng, G.-W. Wu, D. He, H.-P. Peng, A.-L. Liu, X.-H. Xia and W. Chen, *Analyst*, 2015, **140**, 7650.
177 F. Wen, Y. Dong, L. Feng, S. Wang, S. Zhang and X. Zhang, *Anal. Chem.*, 2011, **83**, 1193.
178 C.-W. Wang, Y.-N. Chen, B.-Y. Wu, C.-K. Lee, Y.-C. Chen, Y.-H. Huang and H.-T. Chang, *Anal. Bioanal. Chem.*, 2016, **408**, 287.
179 L.-Y. Chen, C.-C. Huang, W.-Y. Chen, H.-J. Lin and H.-T. Chang, *Biosens. Bioelectron.*, 2013, **43**, 38.
180 Y.-T. Tseng, H.-T. Chang, C.-T. Chen, C.-H. Chen and C.-C. Huang, *Biosens. Bioelectron.*, 2011, **27**, 95.
181 L. Hu, S. Han, S. Parveen, Y. Yuan, L. Zhang and G. Xu, *Biosens. Bioelectron.*, 2012, **32**, 297.
182 W.-Y. Chen, L.-Y. Chen, C.-M. Ou, C.-C. Huang, S.-C. Wei and H.-T. Chang, *Anal. Chem.*, 2013, **85**, 8834.
183 Q. Wen, Y. Gu, L.-J. Tang, R.-Q. Yu and J.-H. Jiang, *Anal. Chem.*, 2013, **85**, 11681.
184 H. Kong, Y. Lu, H. Wang, F. Wen, S. Zhang and X. Zhang, *Anal. Chem.*, 2012, **84**, 4258.
185 S. Xu, X. Lu, C. Yao, F. Huang, H. Jiang, W. Hua, N. Na, H. Liu and J. Ouyang, *Anal. Chem.*, 2014, **86**, 11634.
186 X. M. Qian and S. M. Nie, *Chem. Soc. Rev.*, 2008, **37**, 912.
187 W. E. Smith, *Chem. Soc. Rev.*, 2008, **37**, 955.
188 T. Senapati, D. Senapati, A. K. Singh, Z. Fan, R. Kanchanapally and P. C. Ray, *Chem. Commun.*, 2011, **47**, 10326.
189 H. Wei, K. Rodriguez, S. Renneckar, W. Leng and P. J. Vikesland, *Analyst*, 2015, **140**, 5640.
190 M. Liu, Z. Wang, S. Zong, R. Zhang, D. Zhu, S. Xu, C. Wang and Y. Cui, *Anal. Bioanal. Chem.*, 2013, **405**, 6131.
191 V. V. Thacker, L. O. Herrmann, D. O. Sigle, T. Zhang, T. Liedl, J. J. Baumberg and U. F. Keyser, *Nat. Commun.*, 2014, **5**, 3448.
192 L. Perez-Mayen, J. Oliva, A. Torres-Castro and E. De la Rosa, *Nanoscale*, 2015, **7**, 10249.
193 A. M. Paul, Z. Fan, S. S. Sinha, Y. Shi, L. Le, F. Bai and P. C. Ray, *J. Phys. Chem. C*, 2015, **119**, 23669.
194 D. Senapati, S. S. R. Dasary, A. K. Singh, T. Senapati, H. Yu and P. C. Ray, *Chem. – Eur. J.*, 2011, **17**, 8445.
195 X. Ding, L. Kong, J. Wang, F. Fang, D. Li and J. Liu, *ACS Appl. Mater. Interfaces*, 2013, **5**, 7072.
196 L. Sun, C. Yu and J. Irudayaraj, *Anal. Chem.*, 2007, **79**, 3981.
197 Y. C. Cao, R. Jin and C. A. Mirkin, *Science*, 2002, **297**, 1536.
198 Y. Li, X. Qi, C. Lei, Q. Yue and S. Zhang, *Chem. Commun.*, 2014, **50**, 9907.
199 C.-W. Wang and H.-T. Chang, *Anal. Chem.*, 2014, **86**, 7606.
200 J. F. Li, Y. F. Huang, Y. Ding, Z. L. Yang, S. B. Li, X. S. Zhou, F. R. Fan, W. Zhang, Z. Y. Zhou, Y. WuDe, B. Ren, Z. L. Wang and Z. Q. Tian, *Nature*, 2010, **464**, 392.
201 W. Cai, X. Tang, B. Sun and L. Yang, *Nanoscale*, 2014, **6**, 7954.
202 X. Zhou, F. Zhou, H. Liu, L. Yang and J. Liu, *Analyst*, 2013, **138**, 5832.
203 L. Zhang, H. Ma and L. Yang, *RSC Adv.*, 2014, **4**, 45207.
204 H. Ma, D. Lin, H. Liu, L. Yang, L. Zhang and J. Liu, *Mater. Chem. Phys.*, 2013, **138**, 573.
205 J. F. Li, X. D. Tian, S. B. Li, J. R. Anema, Z. L. Yang, Y. Ding, Y. F. Wu, Y. M. Zeng, Q. Z. Chen, B. Ren, Z. L. Wang and Z. Q. Tian, *Nat. Protoc.*, 2013, **8**, 52.
206 J.-F. Li, S.-Y. Ding, Z.-L. Yang, M.-L. Bai, J. R. Anema, X. Wang, A. Wang, D.-Y. Wu, B. Ren, S.-M. Hou, T. Wandlowski and Z.-Q. Tian, *J. Am. Chem. Soc.*, 2011, **133**, 15922.
207 Z. Liu, S.-Y. Ding, Z.-B. Chen, X. Wang, J.-H. Tian, J. R. Anema, X.-S. Zhou, D.-Y. Wu, B.-W. Mao, X. Xu, B. Ren and Z.-Q. Tian, *Nat. Commun.*, 2011, **2**, 305.
208 J.-F. Li, J. R. Anema, T. Wandlowski and Z.-Q. Tian, *Chem. Soc. Rev.*, 2015, **44**, 8399.
209 J. Yang, Y. Zhao, J. Zhang and C. Zheng, *Environ. Sci. Technol.*, 2014, **48**, 14837.
210 J. Wu, N. Wang, Y. Zhao and L. Jiang, *Nanoscale*, 2015, **7**, 2625.
211 C.-W. Lien, Y.-C. Chen, H.-T. Chang and C.-C. Huang, *Nanoscale*, 2013, **5**, 8227.
212 C.-W. Lien, Y.-T. Tseng, C.-C. Huang and H.-T. Chang, *Anal. Chem.*, 2014, **86**, 2065.
213 Y.-S. Wu, F.-F. Huang and Y.-W. Lin, *ACS Appl. Mater. Interfaces*, 2013, **5**, 1503.

